PAPER

Electronic sideband locking of a broadly tunable 318.6 nm ultraviolet laser to an ultra-stable optical cavity

IOP Publishing Journal of Optics
J. Opt. 19 (2017) 045501 (6pp) https://doi.org/10.1088/2040-8986/aa5a8c

Electronic sideband locking of a broadly tunable 318.6 nm ultraviolet laser to an ultra-stable optical cavity

Jiandong Bai[1,2], Jieying Wang[1,2], Jun He[1,2,3] and Junmin Wang[1,2,3]

[1] State Key Laboratory of Quantum Optics and Quantum Optics Devices, Shanxi University, Tai Yuan 030006, Shan Xi Province, People's Republic of China
[2] Institute of Opto-Electronics, Shanxi University, Tai Yuan 030006, Shan Xi Province, People's Republic of China
[3] Collaborative Innovation Center of Extreme Optics, Shanxi University, Tai Yuan 030006, Shan Xi Province, People's Republic of China

E-mail: wwjjmm@sxu.edu.cn

Received 24 October 2016, revised 22 December 2016
Accepted for publication 11 January 2017
Published 1 March 2017

Abstract

We demonstrate frequency stabilization of a tunable 318.6 nm ultraviolet (UV) laser system using electronic sideband locking. By indirectly changing the frequency of a broadband electro-optic phase modulator, the laser can be continuously tuned over 4 GHz, while a 637.2 nm laser is directly stabilized to a high-finesse ultra-stable optical cavity. The doubling cavity also remains locked to the 637.2 nm light. We show that the tuning range depends mainly on the gain-flattening region of the modulator and the piezo-tunable range of the seed laser. The frequency-stabilized tunable UV laser system is able to compensate for the offset between reference and target frequencies, and has potential applications in precision spectroscopy of cold atoms.

Keywords: electronic sideband locking, frequency offset locking, ultraviolet laser, continuously tunable laser frequency

(Some figures may appear in colour only in the online journal)

1. Introduction

Strong long-range dipole–dipole interactions between highly excited Rydberg atoms lead to the Rydberg blockade mechanism [1–3], which has been used in many practical quantum-based technologies, such as logic gates [4], entanglement between two atoms [5, 6], communications [7] and information processing [1]. In most situations, a two- or three-step excitation is used to address a specific Rydberg state. However, this multi-step excitation inevitably populates intermediate states, producing photon scattering and ac-Stark shifts resulting in low excitation efficiency. These disadvantages can be avoided with single-photon excitation. Tong *et al* [8] and Hankin *et al* [9] have recently demonstrated direct single-photon Rydberg excitation of ^{85}Rb at 297 nm and ^{133}Cs at 319 nm. For single-photon Rydberg excitation of cesium atoms from the $6S_{1/2}$ to an nP (n = 70–100) state, a 318.6 nm ultraviolet (UV) laser should have high power, frequency stabilization, and be continuously tunable over a wide range. Previously [10], we followed the pioneering work of Wineland *et al* [11] to generate a 2.26 W 318.6 nm UV laser starting from two infrared fiber lasers.

A common method to produce a frequency-stabilized tunable laser is to lock it to a fixed optical cavity, or to specific atomic or molecular spectral lines, and then insert one or more acousto-optic modulators (AOMs) in the optical path [12]. A given AOM can create MHz-level shifts, but has a limited bandwidth of dozens of MHz that is only a small fraction of its fixed center frequency. Special AOMs that generate shifts of GHz offer an increased bandwidth (less than several hundred MHz), but their diffraction efficiency is normally very low, and they are very expensive. For a bulk-

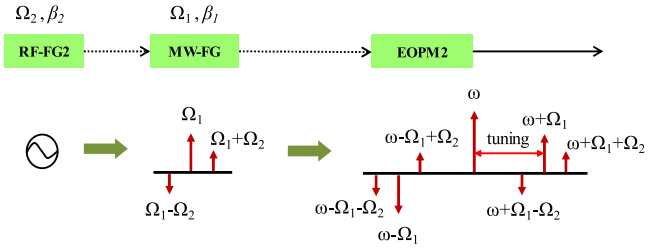

Figure 1. Modulation structures for ESB locking.

type electro-optic phase modulator (EOPM), its maximum bandwidth is only hundreds of MHz. In addition, they need large radio-frequency power consumption. Compared with the bulk-type EOPM and AOM, commercially available fiber-based waveguide-type EOPMs avoid these limitations and have typical bandwidths up to dozens of GHz. Thorpe *et al* [13] proposed sideband locking techniques that involve a few modifications of standard Pound–Drever–Hall (PDH) [14] locking. Based on a waveguide-type EOPM, serrodyne sideband modulation [15, 16] has been recently used for the frequency stabilization of a tunable laser to an optical cavity, with a typical dynamic range of 220 MHz.

Here, we use the electronic sideband (ESB) locking scheme and a high-finesse ultralow expansion (ULE) optical cavity to produce a frequency-stabilized UV laser having a tunable central offset frequency. The ULE cavity is used to stabilize the frequency of two seed lasers, an erbium-doped fiber laser at 1560.5 nm and an ytterbium-doped fiber laser at 1076.9 nm. The erbium-doped laser is directly locked to the ULE cavity, while the locking reference signal for the ytterbium-doped laser comes from the sum frequency beam at 637.2 nm. With a wideband waveguide-type EOPM for this ESB scheme, we obtain a continuous tuning range of 4 GHz in the UV at 318.6 nm, which is much wider than that reported previously [16]. The doubling cavity also remains locked to the 637.2 nm light. The laser system enables single-photon Rydberg excitation of cesium atoms from the $6S_{1/2}$ state to nP (n = 70–100) states.

2. Principle and experimental arrangement

As shown in figure 1, the EOPM2 is driven by a phase-modulated signal. The drive signal produced by a microwave function generator (MW-FG) has a carrier frequency of Ω_1 with a modulation depth of β_1, and is phase modulated by a radio frequency function generator (RF-FG2) at Ω_2 with a modulation depth of β_2. Therefore, the electric field of the laser exiting the EOPM2:

$$E_{\mathrm{ESB}} = E_0 \exp\{\mathrm{i}[\omega t + \beta_1 \sin(\Omega_1 t + \beta_2 \sin \Omega_2 t)]\}, \quad (1)$$

where E_0 is the amplitude of the incident laser at $t = 0$, and ω is the angular frequency of the incoming beam. Using Bessel functions and ignoring contributions from high-order terms, we can expand this expression to first order in β_i ($i = 1, 2$),

$$\begin{aligned} E_{\mathrm{ESB}} &\approx E_0[J_0(\beta_1) + 2\mathrm{i}J_1(\beta_1)\sin \\ &\quad (\Omega_1 t + \beta_2 \sin \Omega_2 t)]\mathrm{e}^{\mathrm{i}\omega t} \\ &\approx E_0 J_0(\beta_1)\mathrm{e}^{\mathrm{i}\omega t} + E_0 J_1(\beta_1) \\ &\quad \times [J_0(\beta_2)\mathrm{e}^{\mathrm{i}(\omega+\Omega_1)t} + J_1(\beta_2)\mathrm{e}^{\mathrm{i}(\omega+\Omega_1+\Omega_2)t} \\ &\quad - J_1(\beta_2)\mathrm{e}^{\mathrm{i}(\omega+\Omega_1-\Omega_2)t}] - E_0 J_1(\beta_1) \\ &\quad \times [J_0(\beta_2)\mathrm{e}^{\mathrm{i}(\omega-\Omega_1)t} - J_1(\beta_2)\mathrm{e}^{\mathrm{i}(\omega-\Omega_1+\Omega_2)t} \\ &\quad + J_1(\beta_2)\mathrm{e}^{\mathrm{i}(\omega-\Omega_1-\Omega_2)t}]. \end{aligned} \quad (2)$$

Here, $J_n(\beta)$ is the n-order Bessel function. The result of the cascaded phase modulation is to split the light into seven different frequency components: a carrier at ω, two sidebands at $\omega \pm \Omega_1$, and four sub-sidebands at $\omega \pm \Omega_1 \pm \Omega_2$. The two components at $\omega + \Omega_1 \pm \Omega_2$ (or $\omega - \Omega_1 \pm \Omega_2$) have opposite phases. Therefore, when the sideband at $\omega + \Omega_1$ or $\omega - \Omega_1$ is locked to a fixed reference cavity, and the carrier and other sidebands are reflected, the ESB error signal is obtained by demodulating the detected signal with the modulation frequency at Ω_2. The frequency discriminant of the locking technique is given by

$$D_{\mathrm{ESB}} = \frac{16FLE_0^2}{c} J_0(\beta_2)J_1(\beta_2)J_1^2(\beta_1), \quad (3)$$

where c is the speed of light in vacuum, L is the optical cavity length, and F is the finesse defined by $F = FSR/\Delta\nu$. Here, $\Delta\nu$ is the full width at half maximum of the cavity signal. When one of the sidebands is near the resonance frequency of the cavity, such as $\omega + \Omega_1 = 2\pi n \cdot FSR$, the carrier frequency of the laser can be tuned by adjusting Ω_1.

A schematic of the experimental arrangement is shown in figure 2. Both infrared lasers (NKT Photonics) seed commercial wide gain bandwidth amplifiers, a 15 W erbium-doped fiber amplifier (EDFA) and a 10 W ytterbium-doped fiber amplifier (YDFA). The boosted laser beams are combined and passed through a 40 mm × 10 mm × 0.5 mm MgO-doped periodically poled lithium niobate crystal with a poling period of 11.80 μm. Previously [17], the crystal was temperature-stabilized at 154.0 °C to produce 8.75 W of 637.2 nm light using single-pass sum frequency generation. The 637.2 nm light is separated by a half-wave plate and a polarization beam splitter cube. The main portion of the 637.2 nm light is frequency doubled to 318.6 nm in a self-designed cavity using a 10 mm × 3 mm × 3 mm Brewster-cut β-BaB_2O_4 (BBO) crystal. A small fraction of its output (~3 mW) is phase modulated by a fiber-coupled waveguide-type EOPM2 (Jenoptik PM635), and then ESB locked to the ULE cavity to stabilize the 1076.9 nm laser.

A waveguide-type EOPM1 (EO-Space PM-0S5-10-PFA-PFA-UL) is placed between the distributed feedback ytterbium-doped fiber laser (DFB-EDFL) and EDFA to produce a set of sidebands at a modulation frequency of 12.6 MHz. The phase-modulated 1560.5 nm laser output is split and one beam is injected into the ULE cavity, and the response is monitored by PD1 in the reflected cavity signal. The driven

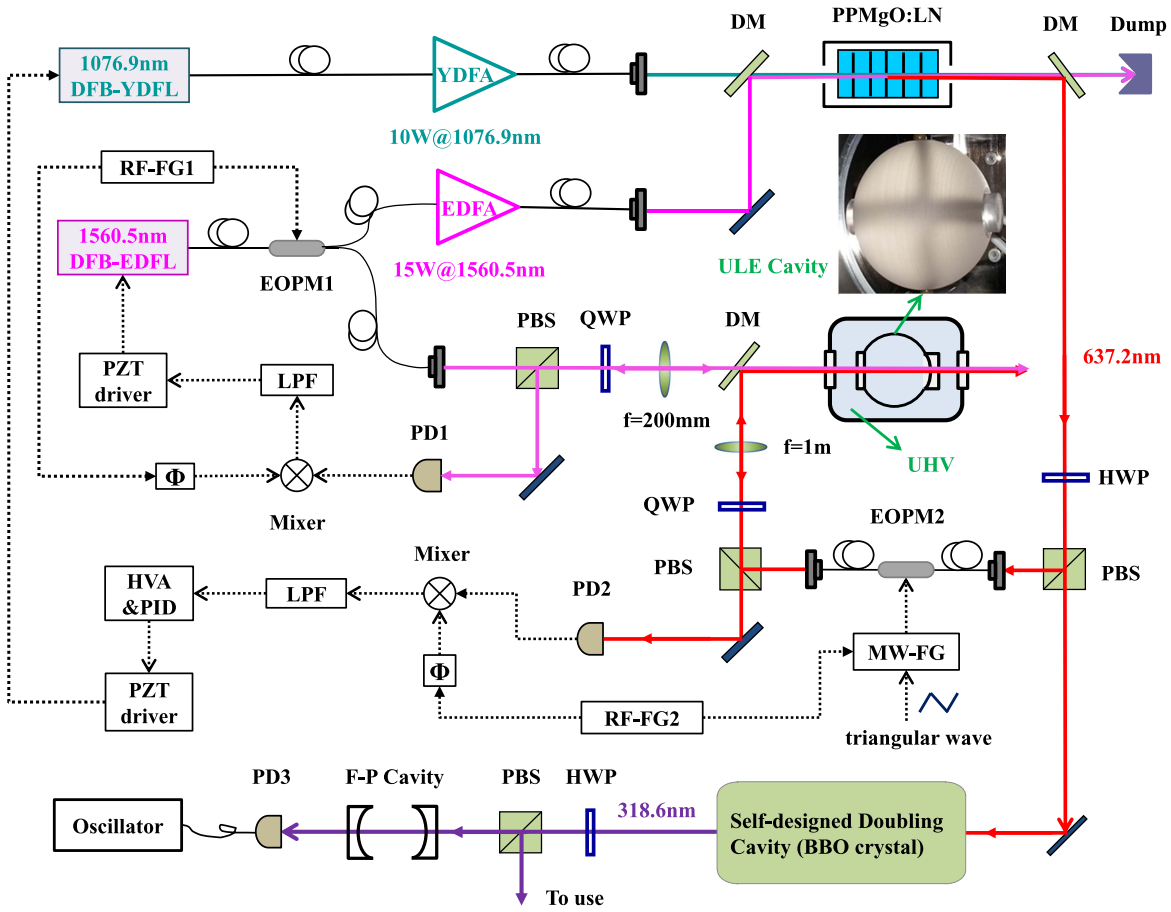

Figure 2. Schematic of the experimental arrangement. Dotted and solid curves represent electronic circuitry and light paths, respectively. DFB-YDFL, distributed feedback ytterbium-doped fiber laser; YDFA, ytterbium-doped fiber amplifier; DFB-EDFL, distributed feedback erbium-doped fiber laser; EDFA, erbium-doped fiber amplifier; DM, dichroic mirror; HWP, half-wave plate; QWP, quarter-wave plate; PBS, polarization beam splitter cube; EOPM, electro-optic phase modulator; RF-FG, radio frequency function generator; MW-FG, microwave function generator; HVA, high-voltage amplifier; PID, proportional-integral-differential controller; LPF, low-pass filter; Φ, phase shift; PD, photodiode detector; ULE, ultralow expansion; UHV, ultra-high vacuum.

signal of a function generator is phase shifted, and then mixed with the detected signal from PD1 to stabilize the 1560.5 nm laser frequency using the PDH technique [14].

The ULE reference cavity is a two-mirror spherical Fabry-Pérot cavity (AT Films) consisting of one plane-plane mirror and one plane-concave mirror with a 500 mm radius of curvature. Both mirrors and the cavity body consist of ULE glass. The mirrors are coated for high reflectivity at 1560.5 and 637.2 nm. The optical cavity is 47.6 mm long, resulting in a 3.145 GHz free spectral range (FSR). With a design similar to that described in [18], the optical cavity is housed in a thermal radiation shield inside a temperature-stabilized and ultra-high vacuum chamber to ensure a uniform temperature that is actively stabilized at the zero crossing of the cavity's coefficient of thermal expansion of 11.113(56) °C. The pressure in the vacuum chamber is kept at $\sim 3 \times 10^{-9}$ Torr using an $8\,\mathrm{L\,s^{-1}}$ ion pump. According to the modulation sideband method, the finesse of the ULE cavity is $3.4(2) \times 10^4$ (FWHM $\sim$ 92 kHz) at 1560.5 nm and $3.0(2) \times 10^4$ (FWHM $\sim$ 105 kHz) at 637.2 nm.

3. Results and discussion

A tunable 318.6 nm laser is required to address various Rydberg states. By slowly changing the DFB-EDFL and DFB-YDFL temperatures over the range 20 °C–50 °C, the 1560.5 and 1076.9 nm infrared seed lasers can be coarsely tuned over 145 and 202 GHz, respectively. This allows coarse tuning ranges of 347 and 694 GHz for the 637.2 and 318.6 nm lasers, respectively. When a tunable sideband of the 637.2 nm laser is locked to the ULE cavity, the offset between the target and reference frequencies depends on the frequency Ω_1 generated by MW-FG (Agilent E8257C). The electronic signal is phase modulated at Ω_2 to produce a pair of sidebands for ESB locking. The PD2 output signal is demodulated with Ω_2 generated by RF-FG2 (Agilent 33250A) via a phase shift. To optimize the error signal, $\Omega_2/2\pi$ is set to 2 MHz with a 10 dBm modulation amplitude. The ESB error signal from the mixer goes into a proportional-integral-differential controller after a 1.9 MHz low-pass filter, and then is fed back to the piezo-electric transducer (PZT) of the 1076.9 nm YDFL to produce frequency-stabilized tunable 637.2 nm laser. The

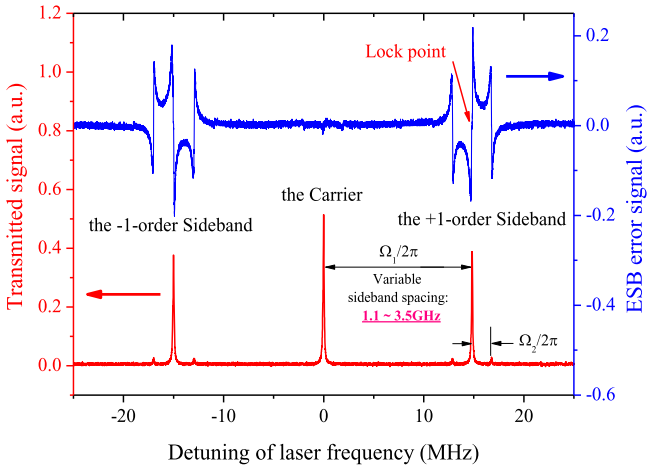

Figure 3. Transmitted signal of the phase-modulated 637.2 nm laser (red curve) incident on the cavity. It is obtained by sweeping the carrier frequency of the 1076.9 nm laser while the 1560.5 nm laser remains locked. The blue curve represents the corresponding ESB error signal. Here, $\Omega_1/2\pi$ and $\Omega_2/2\pi$ are equal to 15 and 2 MHz with RF power consumptions of 14 and 10 dBm, respectively.

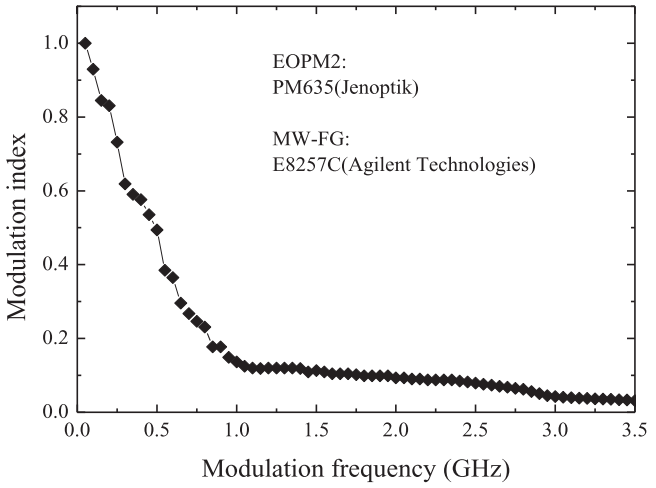

Figure 4. Modulation index dependence on EOPM2 applied modulation frequency. Here the EOPM2 (Jenoptik PM635) is phase modulated by MW-FG (Agilent E8257C).

ESB error signal and the transmitted signal of the phase-modulated 637.2 nm light incident on the ULE cavity are shown in figure 3.

The modulation index of the EOPM2 depends mainly on the applied modulation frequency Ω_1, even if the modulation amplitude is constant (figure 4). The modulation index decreases sharply at modulation frequencies less than 1.1 GHz. Therefore, when sweeping the frequency of the modulator, the gain of the error signal feedback to the PZT of the 1076.9 nm fiber laser is reduced to prevent the 637.2 nm laser frequency from being locked. To obtain a frequency-stabilized tunable 318.6 nm laser, the tuning range of the carrier frequency of the 637.2 nm laser is chosen in the range 1.1–3.5 GHz, which is in the gain-flattening region of the EOPM2 modulation index. In the locked condition, the upper bound of the 637.2 nm laser tuning range is limited by the 3.5 GHz piezo-tuning range of the 1076.9 nm YDFL.

When the carrier frequency of the 1560.5 nm laser and the upper sideband of the 637.2 nm light are locked to the ULE cavity, we tune the carrier frequency of the 637.2 nm light by changing the phase modulation frequency Ω_1. The frequency $\Omega_1/2\pi$ is automatically swept across ~2.4 GHz over the range 1.1–3.5 GHz in a period of 1000 s. Thus, the frequency-tuning rate of the red light is 2.4 MHz s^{-1}. These parameter settings are established by the internal automatic sweep function of MW-FG. As shown in figure 6, if the tuning rate of the 637.2 nm laser frequency is up to hundreds of MHz s^{-1}, where the phase noise of the locking loops is very close to that of the loose lock, it will cause instability in the feedback loops. Therefore, to keep locking loops stable with low phase noise when the laser frequency is swept, a relatively low rate of frequency tuning (less than several MHz s^{-1}) should be used to address the desired state. The tuning range is characterized by a monitor cavity with a 487 MHz FSR. The 637.2 nm laser can be swept across more than four FSRs of the monitor cavity while maintaining lock. Meanwhile, the 318.6 nm UV laser is swept over eight FSRs of the monitor cavity with a FSR of ~500 MHz, indicating that the continuous tuning ranges of the stable 637.2 and 318.6 nm lasers are over 1.95 and 4 GHz, respectively (see figure 5). The tuning range depends mainly on the gain-flattening region of the EOPM and the PZT-tunable range of the 1076.9 nm YDFL. In addition, it is also limited by the RF bandwidth of the EOPM.

When the 1560.5 nm laser is locked to the ULE cavity and the 1076.9 nm laser is free-running and swept by a triangular wave to address the desired Rydberg state, the 637.2 nm laser monitored by the ULE cavity varies about 22 MHz in 30 min because of ambient temperature fluctuations. This frequency stability is not sufficient for Rydberg experiments, but can be improved considerably when the 637.2 nm laser is also locked to the high-finesse ULE cavity.

We characterize the laser frequency stabilization by comparing the power spectral densities (PSDs) of the closed-loop ESB error signal for two cases: a tight lock with optimized parameters and a loose lock where the stabilization is just sufficient to keep the laser frequency on the central slope of the error signal [19]. A nearly linear voltage response for frequency fluctuations is obtained. In figure 6, the experimental data are analyzed with a fast Fourier transform to extract the lower part of the frequency noise power spectrum (10Hz to 20 kHz). It can be seen that the phase noise has been reduced by more than 30 dB within a 17 kHz bandwidth from the crossing point of the two curves. The difference between the PSDs above 17 kHz arises from the response of the error signal to high-frequency deviations beyond its linear region.

If the frequency difference between the sidebands and sub-sidebands of the transmission spectrum is used as a ruler, we lock the upper sideband of the carrier frequency to the zero-crossing point in figure 3. Then we utilize an Rb-stabilized atomic clock to lock the frequencies generated by RF-FG2 and MW-FG to suppress their phase noises. The relative frequency stability is estimated from the slope of the zero-crossing point of the ESB error signal. A 2000 s time trace of the error signal converted from voltage to frequency units is

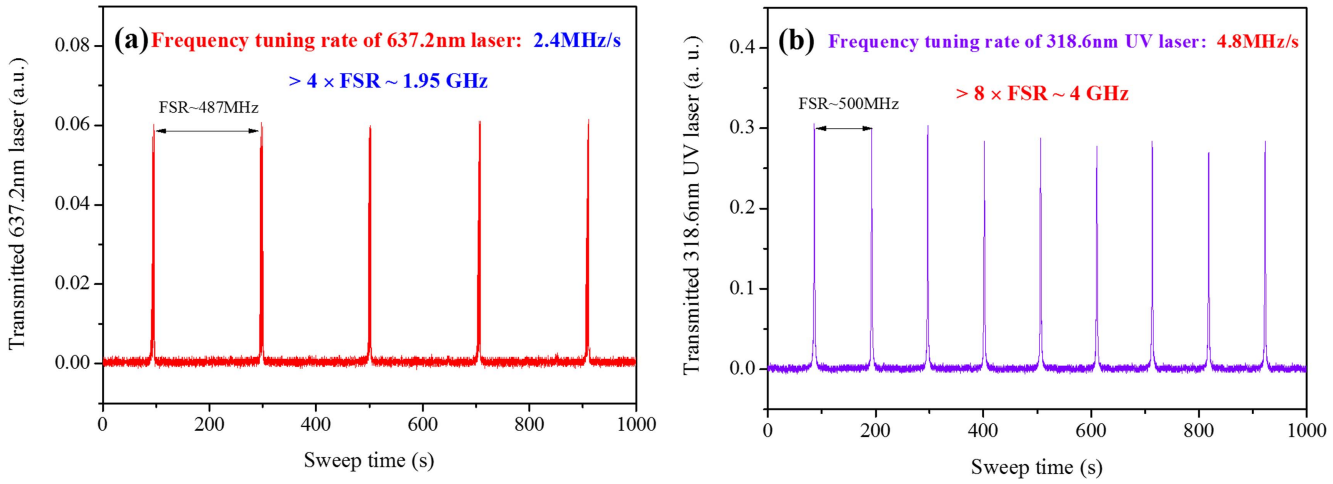

Figure 5. Both the 1560.5 and 637.2 nm lasers are locked to the ULE cavity using the PDH and ESB methods, respectively. By changing the modulation frequency of the EOPM2, after the whole laser system is locked, (a) the carrier frequency of the 637.2 nm light is continuously tuned over 1.95 GHz; (b) simultaneously, the 318.6 nm laser is tuned over 4 GHz when the doubling cavity also remains locked. The tuning ranges of the two lasers are monitored by an optical cavity with a FSR of ~487 and 500 MHz, respectively.

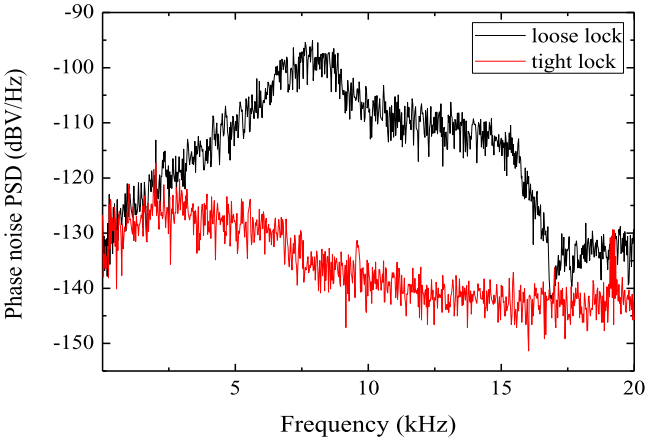

Figure 6. Phase noise power spectral density of the 637.2 nm laser in loose lock (black) and tight lock (red). Noise suppression up to 30 dB is obtained by the ESB tight lock on a ULE cavity relative to a loose lock.

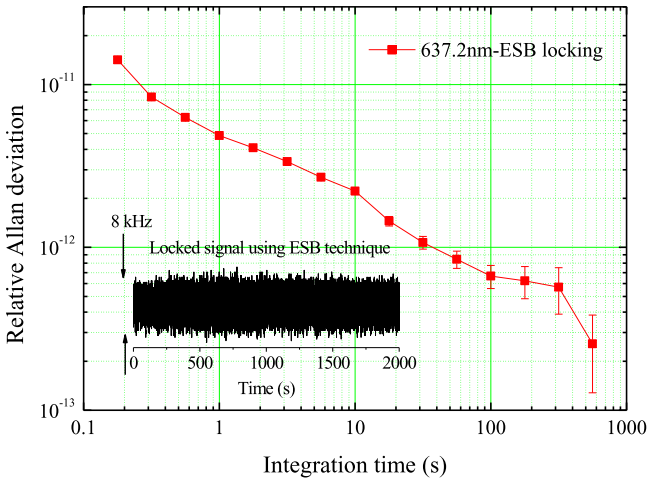

Figure 7. Relative Allan standard deviation plots show the relative frequency instability of the 637.2 nm laser using the ESB (red squares) locking technique. The inset is a time trace of the ESB error signal when the 637.2 nm light is offset-locked.

shown in the inset of figure 7. The relative frequency fluctuations of the locked 637.2 nm laser are below 8 kHz. Figure 7 shows the relative Allan deviation of the 637.2 nm light. Its relative frequency instability is less than 1.5×10^{-11} for interrogation times between 0.1 and over 500 s, corresponding to a frequency deviation of ~7 kHz. Thus, the relative frequency deviation of the 318.6 nm laser is estimated to be less than 15 kHz. It should be emphasized that the relative Allan deviation is derived from the error signal. The measurement is relatively insensitive to frequency variations introduced by tiny variations in cavity length, so it only represents a lower limit of the frequency instability. The Allan deviation should be measured in more detail by the frequency beating of two identical stable laser systems, or optical frequency comb technology, which more accurately reflects laser frequency stability.

Due to the residual amplitude modulation in the EOPM, we can either control the modulator temperature or introduce an intense optical beam to suppress it [20]. To further improve the stability, a fast feedback loop needs to be constructed by inserting an AOM in the 637.2 nm light path [21]. The resulting frequency perturbations of the red light are corrected by feedback on the frequency and amplitude of the AOM, a PZT inside the 1076.9 nm YDFL, and its temperature. In addition, novel materials play an important role in reducing the phase noise of the generated pulse [22, 23], which is possible to improve our fiber laser performance. However, the frequency stability is still sufficient for single-photon Rydberg excitations of cesium atoms [8].

4. Conclusion

In summary, we have demonstrated a continuously tunable frequency-stabilized 318.6 nm UV laser system. A high-finesse ULE optical cavity inside a temperature-stabilized

ultra-high vacuum chamber is used as frequency reference to stabilize 1560.5 and 1076.9 nm seed fiber lasers. Based on a commercial wideband waveguide-type EOPM and the ESB locking technique, the 637.2 nm laser can be continuously tuned over a range of 1.95 GHz while in lock. Meanwhile, the high-stability 318.6 nm UV laser can be continuously tuned over 4 GHz. Further improvements in the tuning range can be achieved by increasing the RF bandwidth of the EOPM, using a widely tunable PZT, and designing the automatic gain control circuit to adjust servo loop parameters. The frequency-stabilized UV laser system with a tunable central offset frequency is important for cesium experiments, including single-photon Rydberg excitation and high precision spectroscopy of Rydberg atoms and their interactions.

Acknowledgments

This project is supported by the National Natural Science Foundation of China (61475091, 11274213, and 61227902) and the National Major Scientific Research Program of China (2012CB921601).

References

[1] Saffman M, Walker T G and Molmer K 2010 Quantum information with Rydberg atoms *Rev. Mod. Phys.* **82** 2313–63

[2] Urban E, Johnson T A, Henage T, Isenhower L, Yavuz D D, Walker T G and Saffman M 2009 Observation of Rydberg blockade between two atoms *Nat. Phys.* **5** 110–4

[3] Barredo D, Ravets S, Labuhn H, Béguin L, Vernier A, Nogrette F, Lahaye T and Browaeys A 2014 Demonstration of a strong Rydberg blockade in three-atom systems with anisotropic interactions *Phys. Rev. Lett.* **112** 183002

[4] Isenhower L, Urban E, Zhang X L, Gill A T, Henage T, Johnson T A, Walker T G and Saffman M 2010 Demonstration of a neutral atom controlled-NOT quantum gate *Phys. Rev. Lett.* **104** 010503

[5] Wilk T, Gaetan A, Evellin C, Wolters J, Miroshnychenko Y, Grangier P and Browaeys A 2010 Entanglement of two individual neutral atoms using Rydberg blockade *Phys. Rev. Lett.* **104** 010502

[6] Zhang X L, Isenhower L, Gill A T, Walker T G and Saffman M 2010 Deterministic entanglement of two neutral atoms via Rydberg blockade *Phys. Rev.* A **82** 030306

[7] Keating T, Goyal K, Jau Y Y, Biedermann G W, Landahl A J and Deutsch I H 2013 Adiabatic quantum computation with Rydberg-dressed atoms *Phys. Rev.* A **87** 052314

[8] Tong D, Farooqi S M, Stanojevic J, Krishnan S, Zhang Y P, Côté R, Eyler E E and Gould P L 2004 Local blockade of Rydberg excitation in an ultra-cold gas *Phys. Rev. Lett.* **93** 063001

[9] Hankin A M, Jau Y Y, Parazzoli L P, Chou C W, Armstrong D J, Landahl A J and Biedermann G W 2014 Two-atom Rydberg blockade using direct 6S to nP excitation *Phys. Rev.* A **89** 033416

[10] Wang J Y, Bai J D, He J and Wang J M 2016 Development and characterization of a 2.2 W narrow-linewidth 318.6 nm ultraviolet laser *J. Opt. Soc. Am.* B **33** 2020–5

[11] Wilson A C, Ospelkaus C, VanDevender A P, Mlynek J A, Brown K R, Leibfried D and Wineland D J 2011 A 750 mW, continuous-wave, solid-state laser source at 313 nm for cooling and manipulating trapped $^{9}Be^{+}$ ions *Appl. Phys.* B **105** 741–8

[12] Bondu F, Fritschel P, Man C and Brillet A 1996 Ultrahigh-spectral-purity laser for the Virgo experiment *Opt. Lett.* **21** 582–4

[13] Thorpe J I, Numata K and Livas J 2008 Laser frequency stabilization and control through offset sideband locking to optical cavities *Opt. Express* **16** 15980–90

[14] Drever R W P, Hall J L, Kowalski F V, Hough J, Ford G M, Munley A J and Wand H 1983 Laser phase and frequency stabilization using an optical resonator *Appl. Phys.* B **31** 97–105

[15] Johnson D M S, Hogan J M, Chiow S-W and Kasevich M A 2010 Broadband optical serrodyne frequency shifting *Opt. Lett.* **35** 745–7

[16] Kohlhaas R, Vanderbruggen T, Bernon S, Bertoldi A, Landragin A and Bouyer P 2012 Robust laser frequency stabilization by serrodyne modulation *Opt. Lett.* **37** 1005–7

[17] Wang J Y, Bai J D, He J and Wang J M 2016 Realization and characterization of single-frequency tunable 637.2 nm high-power laser *Opt. Commun.* **370** 150–5

[18] Leibrandt D R, Bergquist J C and Rosenband T 2013 Cavity-stabilized laser with acceleration sensitivity below $10^{-12}\,g^{-1}$ *Phys. Rev.* A **87** 023829

[19] Leopold T, Schmöger L, Feuchtenbeiner S, Grebing C, Micke P, Scharnhorst N, Leroux I D, Crespo López-Urrutia J R and Schmidt P O 2016 A tunable low-drift laser stabilized to an atomic reference *Appl. Phys.* B **122** 236

[20] Sathian J and Jaatinen E 2013 Reducing residual amplitude modulation in electro-optic phase modulators by erasing photorefractive scatter *Opt. Express* **21** 12309–17

[21] Kessler T, Hagemann C, Grebing C, Legero T, Sterr U, Riehle F, Martin M J, Chen L and Ye J 2012 A sub-40 mHz-linewidth laser based on a silicon single-crystal optical cavity *Nat. Photon.* **6** 687–92

[22] Li X H *et al* 2016 Single-wall carbon nanotubes and graphene oxide-based saturable absorbers for low phase noise mode-locked fiber lasers *Sci. Rep.* **6** 25266

[23] Wu K, Li X H, Wang Y G, Wang Q J, Shum P P and Chen J P 2015 Towards low timing phase noise operation in fiber lasers mode locked by graphene oxide and carbon nanotubes at 1.5 μm *Opt. Express* **23** 501–11